Process integration of microtubes for fluidic applications

Dominic J. Thurmer,[a] Christoph Deneke, Yongfeng Mei, and Oliver G. Schmidt
Max Planck Institute für Festkörperforschung, Heisenbergstr. 1, D-70569 Stuttgart, Germany

(Received 13 September 2006; accepted 10 October 2006; published online 28 November 2006)

Three-dimensional InGaAs/GaAs microtubes are integrated by photolithography into a microfluidic device. The integration process, made possible due to advances in fabricating long, homogeneous rolled-up microtubes, is described in detail. Liquid filling and emptying of individual microtubes, and the final microfluidic device are investigated by video microscopy. The authors find an agreement for their channels with the Washburn equation [Phys. Rev. **17**, 273 (1921)] for filling using a modified capillary pressure fit to experimental conditions. Emptying of a vacuum pumped microfluidic device also qualitatively agrees with theory. The results suggest rolled-up micro- and nanotubes as possible systems to provide fully integrative fluid analysis on a chip. © *2006 American Institute of Physics*. [DOI: 10.1063/1.2396911]

Interest in micro- and nanofluidic devices and lab-on-a-chip research has grown considerably over the last decade.[1–5] Devices, with channels on the size of tens of microns, are being developed for use in a variety of applications such as microreactors, DNA analysis,[6] and micro total analysis systems (μTAS).[7,8] With current techniques, round channel designs are still difficult to realize. Furthermore, smooth channel walls are likely to become increasingly important as the channel size is decreased and the surface-to-volume ratio increases, thus increasing surface effects.[6] More recently, a method of creating round three-dimensional micro- and nano-objects has been established by releasing a strained layer system from its substrate.[9,10] Such rolled-up nanotubes or nanopipelines[11] have been suggested as possible channels in fluidic devices, and filling with dye solution of well-placed nanotubes has been demonstrated.[12,13] The walls of the pipelines are expected to be smooth on the atomic scale because of their evolution from epitaxial layers. Defect-free, rolled-up tubes have been fabricated with large diameter-to-length aspect ratios,[14] can be scaled over several orders of magnitude,[9,15] and can be well positioned on the substrate surface,[12,16] raising hope to integrate them into "top-down" devices on a single chip.[17]

In this letter, we present a linear fluidic device incorporating microtubes connected to two larger reservoirs. A combination of materials including III/V semiconductors, quartz glass, and SU-8 photoresist is utilized in the fabrication of fluidic devices. Semiconductor microtubes in microfluidic devices offer a promising approach to realizing cylindrical geometries with inherently smooth inner surfaces. Advances in postgrowth treatments allow fabrication of microtubes with diameters of approximately 1 μm and lengths that are only limited by the sample size (typically several millimeters) or growth-defect density. Fluid filling and emptying of microtubes are demonstrated in the fabricated devices without the use of a saturated atmosphere. Analysis shows that the fluid dynamics in these tubes can be described using classical theory with a modified capillary pressure.

Rolled-up micro- and nanotubes are created by the selective release of a molecular beam epitaxy grown 14 nm $In_{0.33}Ga_{0.67}As$/14.6 nm GaAs strained bilayer on a 20 nm AlAs sacrificial layer deposited on a GaAs (001) substrate. Before releasing the layers, the samples are patterned by standard photolithography, where the photoresist pattern is used as a mask to etch trenches into the bilayer structure, thus laterally exposing the AlAs sacrificial layer. An isotropic $HBr(50\ vol.\ \%):K_2Cr_2O_7(0.5\ mole/l):CH_3COOH$ (100 vol. %) (2:1:1) solution (BKC-211) is employed for etching. This etchant is known for its isotropic and smooth etching nature in the ternary system.[18] After etching, the samples are exposed to a diluted $HF(50\ vol.\ \%):H_2O$ (1:15) solution, resulting in the selective removal of the AlAs layer and formation of the tubes on the substrate surface as seen in the schematic of Fig. 1(a).

Filling of the tubes is recorded by an optical microscope equipped with corresponding fluorescence filters in combination with fluorescent dye doped liquids. Rhodamine 6G (R6G), in a concentration of 1 mM in ethanol and 10 mM in di-ionized (DI) water is used for filling experiments. Microscope images are captured with a Zeiss Axiocam MRc camera for high-resolution color images, and a Zeiss Axiocam HSm high-speed camera for real time filling.

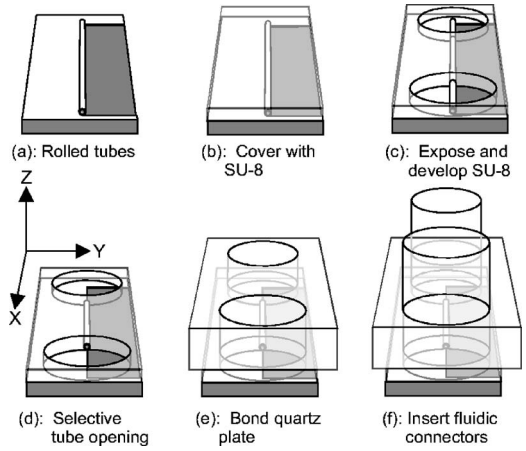

FIG. 1. Schematic drawing of the device processing steps after tube formation. (a) Tube after removing the sacrificial layer. (b) SU-8 protective layer covering the wafer. (c) SU-8 layer after exposure and development. (d) Tube opening using mechanical or chemical methods. (e) Quartz plate bonding onto the SU-8 covered wafer. (f) Insertion of Teflon tubes into the openings in the glass for fluid filling and pumping.

[a]Electronic mail: d.thurmer@fkf.mpg.de

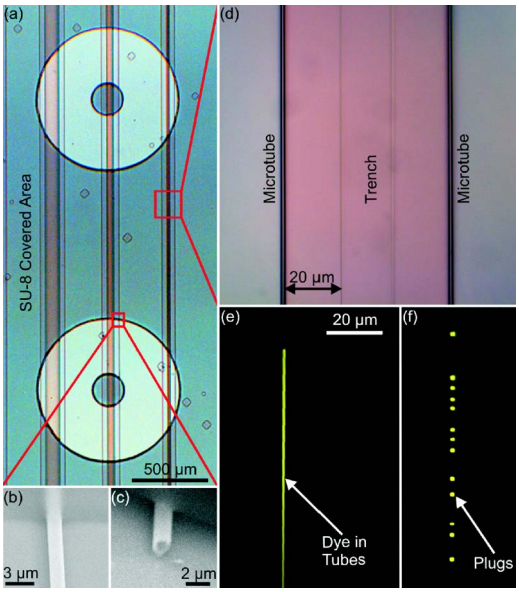

FIG. 2. (Color online) (a) SU-8 covered tubes with six tubes reexposed in the openings for filling. (b) A SEM image of a tube going through an SU-8 interface. (c) A manually opened tube. (d) Light microscope image of two tubes having rolled from a central trench. (e) Fluorescence microscopy image of a tube that is partially filled with a rhodamine 6G fluid. (f) Liquid plug formation in a tube during filling.

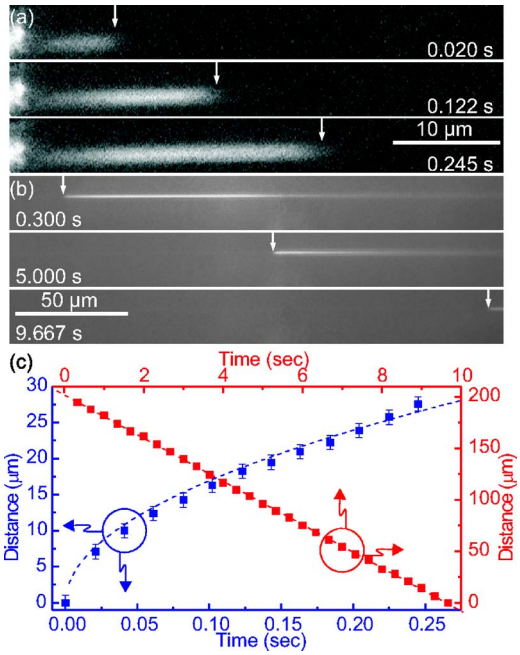

FIG. 3. (Color online) Analysis of filling and emptying of microtube structures. The upper part (a) is a fluorescence filter image selection of a tube being filled with a DI water R6G solution. (b) Emptying of a tube in an SU-8 device. (c) Distance vs time data for filling (blue, bottom-left axes) and emptying (red, top-right axes) of tubes.

To realize a microfluidic device, a process was developed for addressing individual rolled-up microtubes. The process is shown schematically in Figs. 1(a)–1(f). The microtubes are first covered with a protective SU-8 (Microposit) layer, as shown in Fig. 1(b). Circular openings in the SU-8 are created with UV lithography [Fig. 1(c)], also seen in Fig. 2(a). After development, the tubes are either manually opened with a micromanipulator or a BKC-211 etching solution [Fig. 1(d)]. The scanning electron microscope (SEM) image in Fig. 2(b) depicts the interface between the exposed and SU-8 covered tube section (upper part is covered). The SU-8 appears to surround the tube completely, creating a tight seal around it. Figure 2(c) is a SEM image of a tube opened manually with the micromanipulator. Filling experiments of tubes covered by SU-8 verified that there was no fluid flowing along the outside of the tube. Afterwards, a quartz plate containing predrilled holes is also spin coated with an SU-8 layer. The sample with tubes and the SU-8 covered quartz plate are then aligned using a mask aligner and exposed to UV for 15 min [Fig. 1(e)]. Lastly, Teflon tubes are fitted in the openings in the quartz glass for fluid introduction and removal [Fig. 1(f)].

In some experiments, Teflon connectors were not used, but instead tubes were addressed and filled by glass capillaries attached to micromanipulators. An example of such filling is documented in Figs. 2(d)–2(f). Figure 2(d) is a magnified image of Fig. 2(a) showing the uniformity of the tubes over a distance of roughly 100 μm signified by the absence of diffraction colors created by delaminated layers. This homogeneity spans over the full 3 mm shown in Fig. 2(a), resulting in a diameter-to-length aspect ratio of 3000. Figure 2(e) shows a similar structure under an SU-8 layer that is partially filled with an ethanol-R6G solution. The starting point of filling is located below the bottom of the image and the tube is filling towards the top. In Fig. 2(f), a tube section is shown where the liquid has broken into separate liquid plugs. Plug formation[19,20] is determined by the interplay of surface tension of the liquid and the capillary forces present in the channel. Capillary forces, pulling the liquid through the channel, induce a negative Laplace pressure in the liquid and cause the occurrence of bubbles and plug formation.[21]

Analysis of the filling dynamics of rhodamine solutions was carried out both in SU-8 covered structures as well as exposed microtubes. The filling of an exposed microtube with a DI water-R6G solution was recorded and video stills are shown in Fig. 3(a) (for complete video, see Ref. 22). Over three frames the solution fills into a tube to the position marked by the white arrow. The microtube fills over the distance of 25 μm in 25 ms. The frames of the video were analyzed individually to deduce the filling length as a function of time, as shown in Fig. 3(c) (bottom-left axes). We find an initial filling speed of 330 μm/s reducing to 70 μm/s towards the end of the filling video. Further analysis of the data indicates that the fluid follows a quadratic distance-time dependence suggested by Washburn[23] as

$$l^2 = \frac{P_c r^2}{4\eta} t = c^2 t, \quad P_c = \frac{2\gamma_{lv}\cos(\theta)}{r}, \tag{1}$$

where l is the filling distance, γ_{lv} the surface tension of the liquid, η the viscosity, θ the contact angle, r the tube radius, t the time, and P_c the capillary pressure. All parameters are grouped into a single filling coefficient c. With measured values for γ (=70.6 mN/m, using the hanging drop method) and θ (=64°, measured using a horizontal optical microscope), and taking η ($=1\times10^{-3}$ N s/m^2) from literature,[24] the Washburn equation yields $c=2209$ μm s$^{-1/2}$. By fitting our experimental data using a $l=c\sqrt{t}$ dependence, we are able to deduce a filling coefficient of $c=53.5$ μm s$^{-1/2}$. We ascribe this discrepancy to the glass capillary being of roughly the same diameter as the tube and having similar capillary pressures. Therefore, a retarding effect on the filling process is expected, which we express through a calculated modified

capillary pressure, $P_{c(\mathrm{mod})}=P_{c(\mathrm{tube})}-P_{c(\mathrm{glass})}$ $(\theta_{\mathrm{glass}}=51°)$,[25] inserted into Eq. (1). A first estimation calculated using an average capillary radius of 750 nm results in $c=576\ \mu\mathrm{m\ s}^{-1/2}$. Taking r as a fitting parameter to be varied in the range of the average radius for the glass capillaries, we are able to calculate the filling coefficient $c=53.5\ \mu\mathrm{m\ s}^{-1/2}$ with a radius of $r=718$ nm, which is well within the experimental deviation for the capillary radius. Our results indicate that the filling speed sensitively responds to the pressure conditions inside the glass capillary, which depends on its radius, geometry and contact angle. Other possible factors include electro-osmotic counterflow from a streaming potential,[26] a deviation in the dynamic contact angle of water,[27] or an increase in the viscosity of the liquid,[28] none of which would produce a significant deviation and are therefore neglected for the calculations.

Emptying of microtubes was investigated in completed microfluidic devices with a vacuum pump attached by Teflon tubes. With a vacuum of ~30 mbars in one of the openings, vacuum-enhanced evaporation-driven pumping[21,29] is employed and the emptying of the device was investigated by video microscopy (see Ref. 22). The stills in Fig. 3(b) show selected frames of the emptying of a tube. The top frame shows a tube filled with liquid, which then empties over a span of 9 s. (approximately 180 μm, see bottom frame). From the plotted data [Fig. 3(c), top-right axes], a linear dependence between the position of the receding liquid front and time is deduced. From the slope an emptying speed of $v=21\ \mu\mathrm{m/s}$ is estimated. Our results qualitatively agree with the theory presented by Namasivayam *et al.*,[30] suggesting a linear time dependence for evaporation-driven pumping. We point out that the tubes were filled and dried multiple times (not shown), indicating that the structures are robust enough to withstand common microfabrication techniques.

In conclusion, we have shown that rolled-up microtubes can be incorporated into a functional microfluidic device. For measurement of the filling and emptying velocities of tubes we find a qualitative agreement with existing theory. Quantitative comparison of the deduced filling constant to that predicted by the Washburn equation indicated a drastic difference to the expected value for circular geometries, accounted for using a modified capillary pressure. The emptying and refilling of tubes demonstrate that the completed microfluidic devices are fully functional and applicable in many microfluidic device geometries. The robustness of these tubes signifies that further lithographic and deposition steps, such as contact patterning for large scale integration, are certainly feasible. Our results imply that nanotubes integrated into a microfluidic device can serve as model systems to study liquid behavior in round, smooth-walled, two-dimensional confined, micro- and nanometer sized channels.

The authors thank Achim Gueth, Thomas Reindl, and Monika Riek for processing help, Christian Grainer for discussions about SU-8, and Emerson de Souza and Ute Zschieschang for liquid property measurements. The Zeiss Company, Oberkochen, is acknowledged for providing the Axiocam HSm high-speed camera. This work was supported by the BMBF (03N8711) and the European NoE SANDiE.

[1] G. M. Whitesides, Nature (London) **442**, 368 (2006).
[2] J. C. T. Eijkel and A. van den Berg, Microfluid. Nanofluid. **1**, 249 (2005).
[3] I. M. Lazar, J. Grym, and F. Foret, Mass Spectrom. Rev. **25**, 573 (2006).
[4] E. Delamarche, D. Juncker, and H. Schmid, Adv. Mater. (Weinheim, Ger.) **17**, 2911 (2005).
[5] P. J. A. Kenis and A. D. Stroock, MRS Bull. **31**, 87 (2006).
[6] J. O. Tegenfeldt, C. Prinz, H. Cao, R. L. Huang, R. H. Austin, S. Y. Chou, E. C. Cox, and J. C. Sturm, Anal. Bioanal. Chem. **387**, 1678 (2004).
[7] D. R. Reyes, D. Iossifidis, P. A. Auroux, and A. Manz, Anal. Chem. **74**, 2623 (2002).
[8] P. A. Auroux, D. Iossifidis, D. R. Reyes, and A. Manz, Anal. Chem. **74**, 2637 (2002).
[9] V. Y. Prinz, V. A. Seleznev, A. K. Gutakovsky, A. V. Chehovskiy, V. V. Preobrazhenskii, M. A. Putyato, and T. A. Gavrilova, Physica E (Amsterdam) **6**, 828 (2000).
[10] O. G. Schmidt and K. Eberl, Nature (London) **410**, 168 (2001).
[11] O. G. Schmidt and N. Y. Jin-Phillipp, Appl. Phys. Lett. **78**, 3310 (2001).
[12] Ch. Deneke and O. G. Schmidt, Appl. Phys. Lett. **85**, 2914 (2004).
[13] Ch. Deneke and O. G. Schmidt, Physica E (Amsterdam) **23**, 269 (2004).
[14] O. G. Schmidt, Ch. Deneke, S. Kiravitaya, R. Songmuang, H. Heidemeyer, Y. Nakamura, R. Zapf-Gottwick, C. Müller, and N. Y. Jin-Phillipp, IEEE J. Sel. Top. Quantum Electron. **8**, 1025 (2002).
[15] Ch. Deneke, C. Müller, N. Y. Jin-Phillipp, and O. G. Schmidt, Semicond. Sci. Technol. **17**, 1278 (2002).
[16] A. B. Vorob'ev and V. Y. Prinz, Semicond. Sci. Technol. **17**, 614 (2002).
[17] O. G. Schmidt, Ch. Deneke, Y. Nakamura, R. Zapf-Gottwick, C. Müller, and N. Y. Jin-Phillipp, Adv. Solid State Phys. **42**, 231 (2002).
[18] S. Adachi, Y. Noguchi, and H. Kawaguchi, J. Electrochem. Soc. **129**, 1524 (1982).
[19] N. Tas, P. Mela, T. Kramer, J. W. Berenschot, and A. van den Berg, Nano Lett. **3**, 1537 (2003).
[20] A. Han, G. Mondin, N. G. Hegelbach, N. F. de Rooij, and U. Staufer, J. Colloid Interface Sci. **293**, 151 (2005).
[21] N. Goedecke, J. Eijkel, and A. Manz, Lab Chip **2**, 219 (2002).
[22] See EPAPS Document No. E-APPLAB-84-272647 for complete movies. This document can be reached via a direct link in the online article's HTML reference section or via, the EPAPS homepage (http://www.aip.org/pubservs/epaps.html).
[23] E. W. Washburn, Phys. Rev. **17**, 273 (1921).
[24] *CRC Handbook of Chemistry and Physics*, edited by D. R. Lide (CRC Press, Boca Raton, 2001), p. 6–182.
[25] A. Sklodowska, M. Wozniak, and R. Matlakowska, Biol. Proc. Online **1**, 114 (1999).
[26] N. R. Tas, J. Haneveld, H. V. Jansen, M. Elwenspoek, and A. van den Berg, Appl. Phys. Lett. **85**, 3274 (2004).
[27] V. Sobolev, N. Churaev, M. Velarde, and Z. Zorin, J. Colloid Interface Sci. **222**, 51 (1999).
[28] N. V. Churaev, V. D. Sobolev, and Z. M. Zorin, *Special Discussion on Thin Liquid Films and Boundary Layers* (Academic, New York, 1971), p. 213–220.
[29] T. Stiles, R. Fallon, T. Vestad, J. Oakey, D. W. M. Marr, J. Squier, and R. Jimenez, Microfluid. Nanofluid. **1**, 280 (2005).
[30] V. Namasivayam, R. G. Larson, D. T. Burke, and M. A. Burns, J. Micromech. Microeng. **13**, 261 (2003).